Int J Clin Exp Med 2018;11(11):12523-12530
www.ijcem.com /ISSN:1940-5901/IJCEM0076617

Original Article

Exploring the multiple miliary osteoma cutis-related genes by gene expression analysis

Jiaxiao Shi[1*], Ang Li[2*], Zhijian Wei[1*], Yang Liu[1], Cong Xing[1], Hongyu Shi[1], Han Ding[1], Dayu Pan[1], Guangzhi Ning[1], Shiqing Feng[1]

[1]Department of Orthopaedics, Tianjin Medical University General Hospital, Tianjin Neurological Institute, Key Laboratory of Post-Neuroinjury Neuro-Repair and Regeneration in Central Nervous System, Ministry of Education and Tianjin City, No. 154 Anshan Road, Heping District, Tianjin 300052, PR China; [2]Department of Orthopedics, Henan Provincial People's Hospital, Zhengzhou, PR China. [*]Equal contributors.

Received January 30, 2018; Accepted October 12, 2018; Epub November 15, 2018; Published November 30, 2018

Abstract: Objective: The aim of this study was to identify potential genes associated with formation of bone focus in the dermis and subcutis in cases of multiple miliary osteoma cutis (MMOC) through web-available microarrays. Materials and methods: GSE48129 was downloaded from the Gene Expression Omnibus (GEO), and it contained three patients and two controls. The ten samples came from the patients' osteoma affected skin area and unaffected healthy skin area. Differentially expressed genes (DEGs) between the affected group and the unaffected groups were identified by $|logFC| > 1$ and $P < 0.05$. GO and KEGG pathway enrichment analysis were conducted for DEGs by DAVID Functional Annotation Bioinformatics Microarray Analysis. Further, the PPI (protein-protein interaction) network was constructed by the STRING database. Result: We identified 340 upregulated genes and 265 downregulated genes in the MMOC sample. The 605 genes mainly act on G-protein-coupled receptor activity, protein ubiquitination, apoptotic process, protein binding by GO enrichment analysis, and KEGG pathway enrichment, which showed that genes were significantly involved in metabolic pathways and calcium signaling pathways. In the PPI network, ACTA2, PRKACG and PIK3CG appeared at higher degrees. Conclusions: The identified genes may provide a new direction on research focusing on bone formation in MMOC and will lay the foundation for future research.

Keywords: Multiple miliary osteoma cutis (MMOC), differentially expressed genes, microarray, PPI network

Introduction

Osteoma cutis is a benign dermatosis that occurs primarily in the dermis and subcutaneous tissue. It is characterized by imaging and histological confirmation of the formation of bone deposits [1, 2]. Based on these features, patients are classified into four groups: (1) single nodule, (2) plate-like lesion, (3) single or multiple depth lesion, trans-epidermal, and (4) disseminated lesions of various sizes [1]. Analysis of the cases in the previous articles shows that the disease frequently occurs in women and is mostly located on the face, scalp and other specific places [3, 4]. Irrespective of the existence of other existing skin diseases at the site, we divided osteoma into primary and secondary [5]. Multiple miliary osteoma cutis (MMOC) is a type of osteoma cutis, first reported by Virchow in 1864, and it is easily confused with other diseases. It is usually expressed as hard papule on the skin surface [6]. MMOCs are generally visible on patients or are found during the process of diagnosing and treating other issues such as a toothache, so the real epidemiological statistics may not accurately reflect instances of the disease [3]. In the course of disease progression, the size and number of pimples gradually increase, causing discomfort to the face [7]. Therefore, it is necessary to explore the pathogenesis or treatment of MMOC.

At present, the etiology and pathogenesis of MMOC have yet to be elucidated. Discussions on the etiology suggest that the primary MMOC may be related to the Albright's hereditary osteodystrophy (AHO), progressive osseous heteroplasia (POH) and plate-like osteoma cutis (PLOC) or fibrodysplasia ossificans progressive

(FOP), which are all caused by the mutation in the GNAS gene or ACVR1 genes. Mutation of the GNAS reduces the protein Gas, and then Gas induces ossification of the human mesenchymal stem cells. However, unlike GNAS, ACVR1 encodes the BMP4 receptor found in the heterotopic bone [7]. Secondary MMOC occurs after acne, trauma, scar, etc. and is related to chronic inflammation. Some doctors use tretinoin and tetracycline therapy [5, 8]. In pathogenesis, histological samples of the biopsy exhibit smaller bone, surrounded by some lymphocytes, fibrovascular and fewer osteocytes [7]. Currently, ultrasound examinations reveal the bright echoes under permanent focus, and CT scans can confirm the multiple high-density lesions [1, 9]. Some reports mention that there are two possible presentations of the formation of the bone in this disease. One theory illustrates that primitive mesenchymal cells differentiate into osteoblasts and then migrate to inappropriate places. However, only a few people support this point of view. Another theory is that the bone is produced during the transformation of mesenchymal cells into osteoblasts [10].

To explore the key genes in the pathogenesis of MMOC, skin biopsies from three patients and two controls were used to analyze the expression profile. In this study, microarray data had been selected for differential expression genes (DEGs). Subsequently, DEGs were manipulated by gene ontology (GO) and Kyoto Encyclopedia of Genes and Genomes (KEGG) pathway enrichment analysis. Finally, we used the Search Tool for the Retrieval of Interacting Genes (STRING) database to map the protein-protein interaction (PPI) network, aiming to determine the role of DEGs in the development of MMOC.

Materials and methods

Data resource

Gene expression of GSE48129 was downloaded from the Gene Expression Omnibus of NCBI, which was performed on the Affymetrix Human Genome U133 Plus 2.0 Array platform. In the expression profile, they compared patients' osteoma-affected skin areas to both unaffected healthy skin areas and skin from other healthy controls. Next, the gene expression profile was obtained for further analysis.

Identification of DEGs

First, the data were analyzed with the GEO2R, the Gene Expression Omnibus online tool (http://www.ncbi.nlm.nih.gov/geo/geo2r/). Next, we selected 'Define groups' and assigned five samples to each group named the 'affected group' and 'unaffected group'. Third, we selected the 'TOP250' button for calculation usicngs. Fourth, the results were presented as genes tables sorted by significance and we then saved the file [11]. Differentially expressed genes (DEGs) were determined by |logFC| of no less than 1 and t-tests with $P < 0.05$ [12, 13].

GO Terms and KEGG pathways analysis

The DEGs analysis of the GO [14] and KEGG pathways [15] were performed by DAVID (http://david.abcc.ncifcrf.gov/). We limited the *p*-value < 0.05 and the number of genes ≥ 2 to statistically significant. DAVID is an essential foundation for the analysis of high throughput gene function and helps by providing the biological characteristics on genes [16].

Construction of PPI Network and module analysis

STRING (http://string.embl.de/) [15] was applied to construct PPI networks based on significantly up- and downregulated DEGs followed by functional interactions. Then, the data from STRING was entered in the Cytoscape software (version 3.5.1; www.cytoscape.org). The plug-in Molecular Complex Detection (MCODE) was used to screen the modules of PPI network in Cytoscape [13]. The inclusion criteria are as follows: MCODE score > 3, number of nodes > 4.

Samples

From the summary on the GSE48129 content, we were able to study the skin biopsies containing affected skin area and unaffected healthy skin area that were taken from three patients and two controls.

Result

DEG Identification by microarray expression profiling

GSE48129 contained five osteoma samples and five unaffected samples. We used the

Table 1. GO analysis of DEGs in MMOC

Category	Term/gene function	Gene count	%	*p* value
Up-regulate				
GOTERM_BP_FAT	GO: 0042493~response to drug	11	3.75	0.005
GOTERM_BP_FAT	GO: 0043086~negative regulation of catalytic activity	5	1.70	0.014
GOTERM_BP_FAT	GO: 0010466~negative regulation of peptidase activity	3	1.02	0.018
GOTERM_BP_FAT	GO: 0055114~oxidation-reduction process	14	4.78	0.034
GOTERM_MF_FAT	GO: 0050786~RAGE receptor binding	3	1.02	0.008
GOTERM_MF_FAT	GO: 0005542~folic acid binding	3	1.02	0.010
GOTERM_MF_FAT	GO: 0070402~NADPH binding	3	1.02	0.014
GOTERM_CC_FAT	GO: 0005783~endoplasmic reticulum	21	7.17	0.003
GOTERM_CC_FAT	GO: 0005576~extracellular region	32	10.9	0.008
GOTERM_CC_FAT	GO: 0005615~extracellular space	27	0.21	0.014
GOTERM_CC_FAT	GO: 0005789~endoplasmic reticulum membrane	18	6.14	0.037
Down-regulate				
GOTERM_BP_FAT	GO: 0006508~proteolysis	11	4.62	0.021
GOTERM_BP_FAT	GO: 0006954~inflammatory response	9	3.78	0.028
GOTERM_BP_FAT	GO: 0035556~intracellular signal transduction	9	3.78	0.038
GOTERM_MF_FAT	GO: 0042803~protein homodimerization activity	16	6.72	0.004
GOTERM_MF_FAT	GO: 0004222~metalloendopeptidase activity	5	2.10	0.023
GOTERM_MF_FAT	GO: 0004016~adenylate cyclase activity	3	1.26	0.013
GOTERM_CC_FAT	GO: 0015629~actin cytoskeleton	7	2.94	0.016
GOTERM_CC_FAT	GO: 0005887~integral component of plasma membrane	23	9.66	0.012
GOTERM_CC_FAT	GO: 0042995~cell projection	4	1.68	0.032
GOTERM_CC_FAT	GO: 0015629~actin cytoskeleton	7	2.94	0.016

GEO2R, a web page analysis program, to analyze the DEGs. Based on the initial data, we included the inclusion criteria: $P < 0.05$ and $|logFC| \geq 1.0$. Finally, 605 genes were selected, of which 340 were upregulated, and 265 were downregulated.

Go term enrichment analysis

All DEGs were collated and uploaded to the DAVID to pick out the representative GO categories and KEGG pathways. The GO analysis provided results in three parts: biological processes (BP), molecular function (MF) and cell component (CC). In part one (BP), upregulated DEGs were mainly enriched in epidermal development, protein ubiquitination, negative regulation of peptidase activity, etc. The downregulated DEGs were mainly enriched by the negative regulation of the intrinsic apoptotic signaling pathway, ossification, innate immune response, etc. In part two (MF), upregulated DEGs were mainly enriched in NADPH binding, apoptotic processes, protein binding, etc. The downregulated DEGs were mainly enriched in calcium channel activity, protein homodimerization activity, etc. In part three (CC), upregulated DEGs were mainly rich in protease, binding structural molecule activity, endoplasmic reticulum, and ATP binding, and downregulated DEGs have effects on the actin cytoskeleton and postsynaptic membrane (**Table 1**).

KEGG pathway analysis

Table 2 includes the enrichment pathways for upregulation and downregulation of DEGs identified by DAVID. Upregulated DEGs were mainly concentrated in metabolic pathways and in another weakly relative pathways: fatty acid degradation and purine metabolism. However, the downregulated DEGs were enriched in calcium and cAMP signaling pathways. They also participated in other pathways, though these are not mentioned in detail.

Module screening from the PPI network

We uploaded the data to the STRING database, which is able to construct the PPI network.

Table 2. KEGG pathway analysis of DEGs in MMOC

Pathway ID	Name	Gene count	%	*p* value
Up-regulate				
hsa01100	Metabolic pathways	31	10.58	0.0002
hsa00561	Glycerolipid metabolism	5	1.70	0.006
hsa00230	Purine metabolism	8	2.73	0.007
hsa00071	Fatty acid degradation	4	1.37	0.019
Down-regulate				
hsa04024	cAMP signaling pathway	9	3.78	0.0005
hsa04020	Calcium signaling pathway	7	2.94	0.006
hsa05200	Pathways in cancer	9	3.78	0.03
hsa04015	Rap1 signaling pathway	6	2.52	0.046

Table 3. Degree of differentially expressed genes in the protein-protein network

Gene	Degree	Gene	Degree	Gene	Degree
ACTA2	20	MCL1	11	FOXM1	9
PRKACG	19	MTHFD1L	11	FDPS	9
PIK3CG	17	ACSBG1	11	POLR2F	9
SST	15	FASN	11	H2AFX	9
ADCY1	15	ALDH1A2	11	HRH4	9
PTGS2	15	PTGER3	11	GUCY2C	8
ACTL7B	15	AIFM3	11	AGTR1	8
BCL2	14	TYMS	10	PNPLA3	8
PKLR	13	ACOX1	10	HTR1D	8
SREBF1	12	GAL	10	CHRM4	8

Next, the information of PPI network was introduced in the Cytoscape software, and we obtained some nodes of each degree (**Table 3**). In addition, we used the MCODE analysis nodes and edges that were given restrictions. Finally, we selected the top 3 modules and high degree genes for analysis. The genes from module 1 showed the relationship with G protein-coupled receptor signaling pathways; module 2 related to apoptotic signaling pathways; module 3 was associated with the protein ubiquitination (**Table 4**; **Figure 1**).

Discussion

MMOC is a rare disease reported in dermatology, which brings concern to patients. The related literature has reported some methods for treating the disease [9]. Treatment methods include retinoids, tretinoin, tetracycline and estrogens, which were effective against inflammation, but the curative effects were not good [17]. More traumatic treatment methods, such as the needle microincision, YAG or CO_2 lasers are effective, but they also irritated the skin [8, 9]. Understanding the molecular pathogenesis has important implications for better treatment options.

In the MMOC samples, we identified 340 upregulated and 265 downregulated genes. The GO analysis showed that the upregulated DEGs were mainly involved in protein phosphorylation, apoptotic processes and ATP binding. Downregulated DEGs were mainly involved in calcium channel activity, protein binding and innate immune response. Additionally, the KEGG analysis supported the Wnt signaling pathway, pathways in cancer, the PI3K-Akt signaling pathway and the MAPK signaling pathway. These functions and pathways were correlated with reports of the bone and cell proliferation and apoptosis.

We also obtained the 10 most important genes from the PPI network: ACTA2, PRKACG, PIK3CG, SST, ADCY1, PTS2, ACTL1B, Bcl2, PKLR and SREBF1. ACTA2 was the most highly connected. ACTA2 (Alpha 2 actin, smooth muscle), an epithelial-mesenchymal transition-associated gene, was involved in cell motility, structure and integrity, and it also influenced the migration and invasion of tumor cells [18]. Few reports have described the ACTA2's function in bone metabolism. Benjamin H. Mullin reported, in the osteoclast-like cells and osteoblast-like cells, ACTA2 might be regulated by the RhoA signaling pathway [19]. Furthermore, ACTA2 is the main expression protein of blood vessels in the plaque-deposited Alzheimer's mouse model which may be associated with CD105 positive cells that were mentioned by initial researcher [20]. In addition, as the marker of osteoprogenitor cells, which undergo osteogenic differentiation induced by BMP-2 in vivo and in vitro [21], and α-SMA-positive MSCs exhibited differentiation potential limited to osteogenesis [22]. The second gene, PRKACG, which encodes the cAMP-dependent protein kinase catalytic subunity, is usually cor-

Table 4. Top3 modules from Protein-protein interaction network constituted by DEGs and the enriched pathways respectively

Cluster	Score	Nodes	Edges	Node IDs	Enriched pathways
1	9	9	36	PTGER3, CXCL5, ADCY1, S1PR3, HTR1D, HRH4, GAL, CHRM4, SST	1. G-protein coupled receptor signaling pathway 2. Adenylate cyclase-modulating G-protein coupled receptor signaling pathway 3. Cell-cell signaling
2	5.6	6	14	PIK3CG, MCL1, PI3, BCL2, BCL2L11, PTGS2	1. Positive regulation of intracellular signal transduction 2. Extrinsic apoptotic signaling pathway in absence of ligand 3. Apoptotic mitochondrial changes
3	5	5	10	TRAF7, HECTD2, ASB12, FBXO40, RNF14	1. Protein ubiquitination

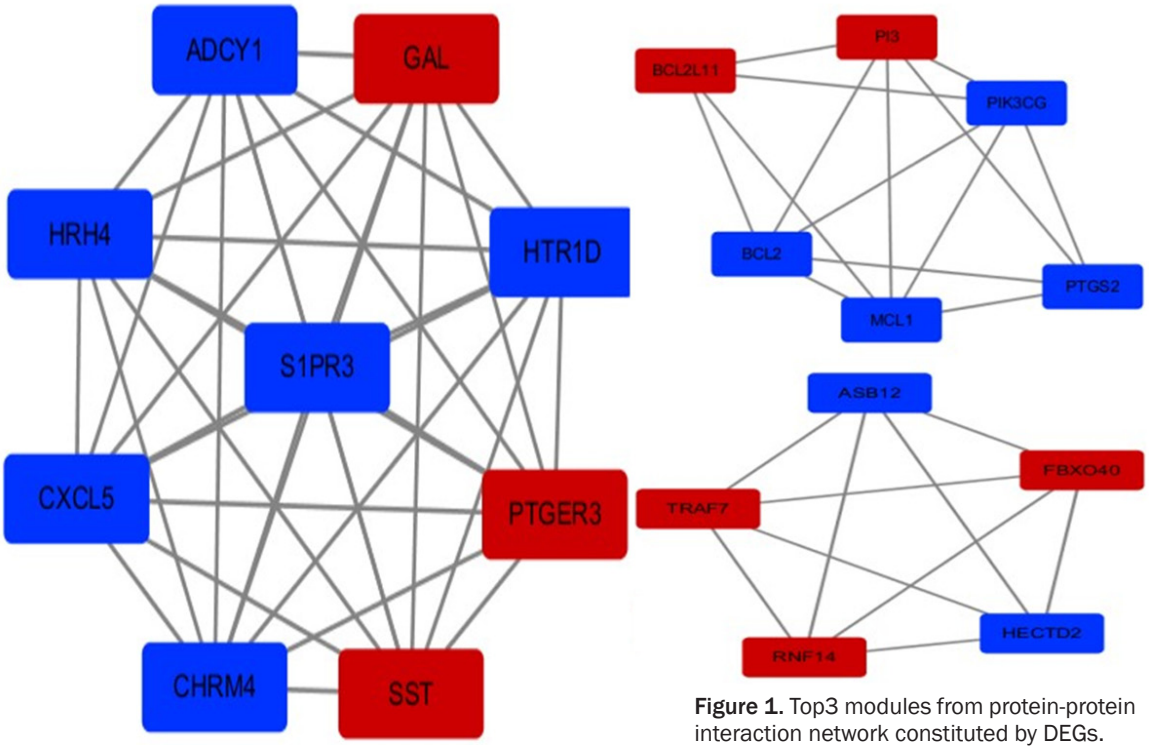

Figure 1. Top3 modules from protein-protein interaction network constituted by DEGs.

related with platelet-associated disease [23, 24]. Zhang S reported that it might affect the regulation of cell function and improve proliferation through NF-rB pathway [25]. The third gene, PIK3CG, plays a key role in the PI3K signaling pathway. PI3k-Akt/PKB is a pathway involved in cell survival, proliferation and metastasis, and PI3K/Akt/mTOR is relevant for psoriasis [26]. PIK3CG as a direct downstream target of miR-502 in hepatocellular carcinoma cells interacts with G protein-coupled receptors during the proliferation of hepatocellular carcinoma cells [27]. Additionally, PIK3CG ubiquitination occurring during apoptosis in cervical cancer cells is mediated through the PIK3 pathway and is also related to the formation of carotid plaques [28, 29]. Apoptosis of osteoblasts can be regulated by the VDR/PI3K/Akt survival pathway [30]. SST is a regulatory peptide and has an anti-proliferative and pro-apoptotic effects [31, 32]. It has 5 receptors that are typical G-protein-coupled receptors that act through the MAPK pathway or methylation in the cancer [33]. ADCY1 is also mediated by G-protein-coupled receptors in cell growth and is an isoform of adenylyl cyclase that synthetizes cAMP. cAMP plays an extended role in cell functions as a second messenger [34]. In the proteomic analysis of osteosarcoma tissue and bone tumors, ADCY1 is downregulated [35]. The PTGS2 gene encodes the cyclo-oxygenase2 (COX2), which mainly induces the inflammatory response. Inhibiting COX2 blocks the mitogenic effect in osteoblasts, which metasta-

size to bone and growth in cancer [36-38]. BMP-2 can regulated COX-2 to influence the formation of osteoclast 10334922. ACTL7B is an actin-like gene of ARP family involving similar cellular processes has been found in the testis and prostate. It has a site for cAMP/cGMP-dependent phosphorylation [39]. Bcl2, which is overexpressed in the osteoblast, inhibits cell differentiation [40]. However, in the osteoclast, Bcl2 plays the anti-apoptotic role [41], so down-regulation of the Bcl2 can promote the bone formation. PKLR mainly encodes pyruvate kinase, the lack of which leads to hereditary nonspherocytic hemolytic anemia [42]. In addition, PKLR can accumulate the glutathione and affect processes related to the migration of colon cancer [43]. SREBP transcription factors are major regulators of lipid metabolism and are closely related to cell growth and induces epithelial-mesenchymal transition [44-46]. For other genes, the most upregulated are IGHV4-31, IGHM, IGHG2, and IGHG1, which are immunoglobulin-related genes that may be associated with secondary MMOC. The most down-regulated gene, FOXC2, is a transcriptional regulator of intermediate transformation during developmental epithelial-mesenchymal transition (EMT) processes, which regulates the expression of α-SMA and vimentin and affects cell migration and invasion [47, 48]. More importantly, there are articles demonstrating that Foxc2 stimulates osteoblast differentiation in mesenchymal and preosteoblasts [49].

Conclusions

Our results highlight the importance of DEGs, which may highlight some important elements of the MMOC, with some being related to the tumor and some being related to G-protein-coupled receptors. G-protein α can induce the osteoblastic metaplasia of mesenchymal cells [7]. New genes have been found to be related to MMOC, but the function of these genes remains to be elucidation. These discoveries may provide hope outside of the traditional theory for treatment.

Acknowledgements

The present study was supported by the State Key Program of National Nature Science Foundation of China (grant No. 81330042), International Cooperation Program of National Natural Science Foundation of China (81-620108018), National Natural Science Foundation of China (81472070, 81772342), National Natural Science Foundation of China (81702147).

Disclosure of conflict of interest

None.

Address correspondence to: Shiqing Feng and Jingcheng Sun, Department of Orthopaedics, Tianjin Medical University General Hospital, No. 154 Anshan Road, Heping District, Tianjin 300052, PR China. Tel: +8602288366139; Fax: +8602288-366139; E-mail: sqfeng@tmu.edu.cn (SQF); ningguangzhi@foxmail.com (JCS)

References

[1] Safi Y, Valizadeh S, Vasegh S, Aghdasi MM, Shamloo N and Azizi Z. Prevalence of osteoma cutis in the maxillofacial region and classification of its radiographic pattern in cone beam CT. Dermatol Online J 2016; 22.

[2] Caravaglio JV, Gupta R and Weinstein D. Multiple miliary osteoma cutis of the face associated with albright hereditary osteodystrophy in the setting of acne vulgaris: a case report. Dermatol Online J 2017; 23.

[3] Caliskan A and Celenk P. Imaging a dermatosis with dental radiographs: a case report of facial osteoma cutis. Quintessence Int 2016; 47: 705-709.

[4] Painsi C, Tarmann R, Georg Wurtz F, Malle P, Wolf P, Hugel R and Lange-Asschenfeldt B. Multiple miliary osteoma cutis of the scalp. J Dtsch Dermatol Ges 2015; 13: 1185-1187.

[5] Ma HJ, Jia CY, Yang Y, Song LJ, Hu R and Li TH. Primary multiple miliary osteoma cutis: an unusual Chinese case. Int J Dermatol 2014; 53: 73-75.

[6] Kim SY, Park SB, Lee Y, Seo YJ, Lee JH and Im M. Multiple miliary osteoma cutis: treatment with CO(2) laser and hook. J Cosmet Laser Ther 2011; 13: 227-230.

[7] Myllyla RM, Haapasaari KM, Palatsi R, Germain-Lee EL, Hagg PM, Ignatius J and Tuukkanen J. Multiple miliary osteoma cutis is a distinct disease entity: four case reports and review of the literature. Br J Dermatol 2011; 164: 544-552.

[8] Cohen AD, Chetov T, Cagnano E, Naimer S and Vardy DA. Treatment of multiple miliary osteoma cutis of the face with local application of tretinoin (all-trans-retinoic acid): a case report and review of the literature. J Dermatolog Treat 2001; 12: 171-173.

[9] Baskan EB, Turan H, Tunali S, Toker SC, Adim SB and Bolca N. Miliary osteoma cutis of the

face: treatment with the needle microincision-extirpation method. J Dermatolog Treat 2007; 18: 252-254.
[10] Altman JF, Nehal KS, Busam KJ and Halpern AC. Treatment of primary miliary osteoma cutis with incision, curettage, and primary closure. J Am Acad Dermatol 2001; 44: 96-99.
[11] Zhang Y, Fang L, Zang Y and Xu Z. Identification of core genes and key pathways via integrated analysis of gene expression and DNA methylation profiles in bladder cancer. Med Sci Monit 2018; 24: 3024-3033.
[12] Liu X, Qu J, Xue W, He L, Wang J, Xi X, Liu X, Yin Y and Qu Y. Bioinformatics-based identification of potential microRNA biomarkers in frequent and non-frequent exacerbators of COPD. Int J Chron Obstruct Pulmon Dis 2018; 13: 1217-1228.
[13] Zhou L, Du Y, Kong L, Zhang X and Chen Q. Identification of molecular target genes and key pathways in hepatocellular carcinoma by bioinformatics analysis. Onco Targets Ther 2018; 11: 1861-1869.
[14] Ashburner M, Ball CA, Blake JA, Botstein D, Butler H, Cherry JM, Davis AP, Dolinski K, Dwight SS, Eppig JT, Harris MA, Hill DP, Issel-Tarver L, Kasarskis A, Lewis S, Matese JC, Richardson JE, Ringwald M, Rubin GM and Sherlock G. Gene ontology: tool for the unification of biology. The gene ontology consortium. Nat Genet 2000; 25: 25-29.
[15] Nakaya A, Katayama T, Itoh M, Hiranuka K, Kawashima S, Moriya Y, Okuda S, Tanaka M, Tokimatsu T, Yamanishi Y, Yoshizawa AC, Kanehisa M and Goto S. KEGG OC: a large-scale automatic construction of taxonomy-based ortholog clusters. Nucleic Acids Res 2013; 41: D353-357.
[16] Huang da W, Sherman BT and Lempicki RA. Systematic and integrative analysis of large gene lists using DAVID bioinformatics resources. Nat Protoc 2009; 4: 44-57.
[17] Smith CG and Glaser DA. Treatment of multiple miliary osteoma cutis with tretinoin gel. J Am Acad Dermatol 1999; 41: 500.
[18] Vastrad B, Vastrad C, Tengli A and Iliger S. Identification of differentially expressed genes regulated by molecular signature in breast cancer-associated fibroblasts by bioinformatics analysis. Arch Gynecol Obstet 2018; 297: 161-183.
[19] Mullin BH, Mamotte C, Prince RL and Wilson SG. Influence of ARHGEF3 and RHOA knockdown on ACTA2 and other genes in osteoblasts and osteoclasts. PLoS One 2014; 9: e98116.
[20] Hutter-Schmid B and Humpel C. Alpha-smooth muscle actin mRNA and protein are increased in isolated brain vessel extracts of alzheimer mice. Pharmacology 2016; 98: 251-260.
[21] Matthews BG, Torreggiani E, Roeder E, Matic I, Grcevic D and Kalajzic I. Osteogenic potential of alpha smooth muscle actin expressing muscle resident progenitor cells. Bone 2016; 84: 69-77.
[22] Talele NP, Fradette J, Davies JE, Kapus A and Hinz B. Expression of alpha-smooth muscle actin determines the fate of mesenchymal stromal cells. Stem Cell Reports 2015; 4: 1016-1030.
[23] Lambert MP. Update on the inherited platelet disorders. Curr Opin Hematol 2015; 22: 460-466.
[24] Beebe SJ, Oyen O, Sandberg M, Froysa A, Hansson V and Jahnsen T. Molecular cloning of a tissue-specific protein kinase (C gamma) from human testis--representing a third isoform for the catalytic subunit of cAMP-dependent protein kinase. Mol Endocrinol 1990; 4: 465-475.
[25] Zhang S, Li L, Huang Z, Xin X and Xiao B. Application of genome-wide genechip for screening and identifying genes related to CD133(+) CD200(+) colorectal cancer stem cells. Nan Fang Yi Ke Da Xue Xue Bao 2013; 33: 1787-1791.
[26] Chamcheu JC, Adhami VM, Esnault S, Sechi M, Siddiqui IA, Satyshur KA, Syed DN, Dodwad SM, Chaves-Rodriquez MI, Longley BJ, Wood GS and Mukhtar H. Dual inhibition of PI3K/Akt and mTOR by the dietary antioxidant, delphinidin, ameliorates psoriatic features in vitro and in an imiquimod-induced psoriasis-like disease in mice. Antioxid Redox Signal 2017; 26: 49-69.
[27] Chen S, Li F, Chai H, Tao X, Wang H and Ji A. miR-502 inhibits cell proliferation and tumor growth in hepatocellular carcinoma through suppressing phosphoinositide 3-kinase catalytic subunit gamma. Biochem Biophys Res Commun 2015; 464: 500-505.
[28] Chen YJ, Kay N, Yang JM, Lin CT, Chang HL, Wu YC, Fu CF, Chang Y, Lo S, Hou MF, Lee YC, Hsieh YC and Yuan SS. Total synthetic protoapigenone WYC02 inhibits cervical cancer cell proliferation and tumour growth through PIK3 signalling pathway. Basic Clin Pharmacol Toxicol 2013; 113: 8-18.
[29] Wang G, Kuai D, Yang Y, Yang G, Wei Z and Zhao W. Screening of potential gene markers for predicting carotid atheroma plaque formation using bioinformatics approaches. Mol Med Rep 2017; 15: 2039-2048.
[30] Zhang X and Zanello LP. Vitamin D receptor-dependent 1 alpha, 25(OH)2 vitamin D3-induced anti-apoptotic PI3K/AKT signaling in osteoblasts. J Bone Miner Res 2008; 23: 1238-1248.
[31] Leiszter K, Sipos F, Galamb O, Krenacs T, Veres G, Wichmann B, Furi I, Kalmar A, Patai AV, Toth

K, Valcz G, Tulassay Z and Molnar B. Promoter hypermethylation-related reduced somatostatin production promotes uncontrolled cell proliferation in colorectal cancer. PLoS One 2015; 10: e0118332.

[32] War SA and Kumar U. Coexpression of human somatostatin receptor-2 (SSTR2) and SSTR3 modulates antiproliferative signaling and apoptosis. J Mol Signal 2012; 7: 5.

[33] Zhou G, Sinnett-Smith J, Liu SH, Yu J, Wu J, Sanchez R, Pandol SJ, Abrol R, Nemunaitis J, Rozengurt E and Brunicardi FC. Down-regulation of pancreatic and duodenal homeobox-1 by somatostatin receptor subtype 5: a novel mechanism for inhibition of cellular proliferation and insulin secretion by somatostatin. Front Physiol 2014; 5: 226.

[34] Ludwig MG and Seuwen K. Characterization of the human adenylyl cyclase gene family: cDNA, gene structure, and tissue distribution of the nine isoforms. J Recept Signal Transduct Res 2002; 22: 79-110.

[35] Li Y, Liang Q, Wen YQ, Chen LL, Wang LT, Liu YL, Luo CQ, Liang HZ, Li MT and Li Z. Comparative proteomics analysis of human osteosarcomas and benign tumor of bone. Cancer Genet Cytogenet 2010; 198: 97-106.

[36] Wang D, Xia D and Dubois RN. The crosstalk of PTGS2 and EGF signaling pathways in colorectal cancer. Cancers (Basel) 2011; 3: 3894-3908.

[37] Pollari S, Leivonen SK, Perala M, Fey V, Kakonen SM and Kallioniemi O. Identification of microRNAs inhibiting TGF-beta-induced IL-11 production in bone metastatic breast cancer cells. PLoS One 2012; 7: e37361.

[38] Naot D, Chhana A, Matthews BG, Callon KE, Tong PC, Lin JM, Costa JL, Watson M, Grey AB and Cornish J. Molecular mechanisms involved in the mitogenic effect of lactoferrin in osteoblasts. Bone 2011; 49: 217-224.

[39] Chadwick BP, Mull J, Helbling LA, Gill S, Leyne M, Robbins CM, Pinkett HW, Makalowska I, Maayan C, Blumenfeld A, Axelrod FB, Brownstein M, Gusella JF and Slaugenhaupt SA. Cloning, mapping, and expression of two novel actin genes, actin-like-7A (ACTL7A) and actin-like-7B (ACTL7B), from the familial dysautonomia candidate region on 9q31. Genomics 1999; 58: 302-309.

[40] Moriishi T, Maruyama Z, Fukuyama R, Ito M, Miyazaki T, Kitaura H, Ohnishi H, Furuichi T, Kawai Y, Masuyama R, Komori H, Takada K, Kawaguchi H and Komori T. Overexpression of Bcl2 in osteoblasts inhibits osteoblast differentiation and induces osteocyte apoptosis. PLoS One 2011; 6: e27487.

[41] Lee JY and Lee NK. Up-regulation of cyclin D1 and Bcl2A1 by insulin is involved in osteoclast proliferation. Life Sci 2014; 114: 57-61.

[42] van Wijk R, Huizinga EG, van Wesel AC, van Oirschot BA, Hadders MA and van Solinge WW. Fifteen novel mutations in PKLR associated with pyruvate kinase (PK) deficiency: structural implications of amino acid substitutions in PK. Hum Mutat 2009; 30: 446-453.

[43] Nguyen A, Loo JM, Mital R, Weinberg EM, Man FY, Zeng Z, Paty PB, Saltz L, Janjigian YY, de Stanchina E and Tavazoie SF. PKLR promotes colorectal cancer liver colonization through induction of glutathione synthesis. J Clin Invest 2016; 126: 681-694.

[44] Bengoechea-Alonso MT and Ericsson J. The phosphorylation-dependent regulation of nuclear SREBP1 during mitosis links lipid metabolism and cell growth. Cell Cycle 2016; 15: 2753-2765.

[45] Li Y, Zhang J, He J, Zhou W, Xiang G and Xu R. MicroRNA-132 cause apoptosis of glioma cells through blockade of the SREBP-1c metabolic pathway related to SIRT1. Biomed Pharmacother 2016; 78: 177-184.

[46] Wang Y, Wang H, Zhao Q, Xia Y, Hu X and Guo J. PD-L1 induces epithelial-to-mesenchymal transition via activating SREBP-1c in renal cell carcinoma. Med Oncol 2015; 32: 212.

[47] Golden D and Cantley LG. Casein kinase 2 prevents mesenchymal transformation by maintaining Foxc2 in the cytoplasm. Oncogene 2015; 34: 4702-4712.

[48] Hader C, Marlier A and Cantley L. Mesenchymal-epithelial transition in epithelial response to injury: the role of Foxc2. Oncogene 2010; 29: 1031-1040.

[49] Kim SH, Cho KW, Choi HS, Park SJ, Rhee Y, Jung HS and Lim SK. The forkhead transcription factor Foxc2 stimulates osteoblast differentiation. Biochem Biophys Res Commun 2009; 386: 532-536.